

# Evidence of hybridization states at the donor/acceptor interface: case of *m*-MTDATA/PPT

Teng Zhang<sup>11,1\*</sup>, Tingting Wang<sup>1</sup>, Cesare Grazioli<sup>2</sup>, Ambra Guarnaccio<sup>3</sup>, Iulia Emilia Brumboiu<sup>4</sup>, Fredrik O L Johansson<sup>5,6,7</sup>, Klára Beranová<sup>8,9</sup>, Marcello Coreno<sup>3</sup>, Monica de Simone<sup>2</sup>, Barbara Brena<sup>10</sup>, Liwei Liu<sup>1</sup>, Yeliang Wang<sup>1</sup> and Carla Puglia<sup>5</sup>

\* [teng.zhang@bit.edu.cn](mailto:teng.zhang@bit.edu.cn)

<sup>1</sup> School of Integrated Circuits and Electronics, MIIT Key Laboratory for Low-Dimensional Quantum Structure and Devices, Beijing Institute of Technology, 100081 Beijing, People's Republic of China

<sup>2</sup> IOM-CNR, Laboratorio TASC, Sincrotrone Trieste, 34149 Trieste, Italy

<sup>3</sup> ISM-CNR, Istituto di Struttura della Materia, 85050 Tito Scalo (Pz) and 34149 Trieste (Ts), Italy

<sup>4</sup> Department of Chemistry, Pohang University of Science and Technology (POSTECH), 37673 Pohang, Republic of Korea

<sup>5</sup> Division of X-ray Photon Science, Department of Physics and Astronomy, Uppsala University, Box 516, SE-751 20 Uppsala, Sweden

<sup>6</sup> Division of Applied Physical Chemistry, Department of Chemistry, KTH Royal Institute of Technology, 10044 Stockholm, Sweden

<sup>7</sup> Institut des Nanosciences de Paris, UMR CNRS 7588, Sorbonne Université, F-75005 Paris, France

<sup>8</sup> Elettra-Sincrotrone Trieste S. C. p. A., Strada Statale 14, km 163.5, Basovizza, 34149 Trieste, Italy

<sup>9</sup> FZU-Institute of Physics of the Czech Academy of Sciences, 18221 Prague, Czech Republic

<sup>10</sup> Division of Materials Theory, Department of Physics and Astronomy, Uppsala University, Box 516, SE-751 20 Uppsala, Sweden

## Abstract

We performed a spectroscopic study on the *m*-MTDATA (donor) and PPT (acceptor) molecular vertical heterostructure. The electronic properties of the donor/acceptor interface have been comprehensively characterized by synchrotron radiation-based photoelectron spectroscopy and near-edge x-ray absorption fine structure. The spectroscopic results reveal the existence of new hybridization states in the original molecular energy gap, likely attributed to the interaction between the donor and the acceptor molecules at the interface. Such hybridized states can have a significant impact on the charge transport in organic electronic devices based on donor–acceptor molecules and can explain the increased efficiency of device using such molecules.

## 1. Introduction

31 Charge transfer/separation occurring at the interface plays a key role in organic optoelectronic devices, such as organic light-  
32 emitting diodes (OLEDs), organic photovoltaics (OPVs), as well as the solid dye-sensitized solar cell developed recently [1–5].  
33 Blends of electron-donating and electron-accepting molecules constitute the active layer of OPVs and their use in OLEDs has  
34 been shown to improve the performance [6–10]. Therefore, understanding the electronic structure at the donor/acceptor  
35 heterostructure is the focus of intense research interest for developing efficient optoelectronic devices [11–15].  
36 Fundamental studies focused on modifications of the electronic structure of the donor/acceptor components due to the interface  
37 are crucial to understand the charge separation processes at organic/inorganic and organic/organic heterojunctions for new  
38 developments and device optimizations [16]. We focus the present study on *in situ* samples grown under controlled ultra-high  
39 vacuum conditions to define a model system for studying these processes.  
40 *m*-MTDATA (4,4',4''-Tris (N-3-methylphenyl-N-phenyl-amino) triphenylamine, C<sub>57</sub>H<sub>48</sub>N<sub>4</sub>, shown in figure 1(a)) belongs to a  
41 group of molecules called 'starburst  $\pi$ -conjugated molecules', widely used in organic optoelectronic devices, like OLEDs and  
42 OPVs. The good electron-donating and charge-transport properties of *m*-MTDATA are largely given by its building block  
43 triphenylamine (TPA), involving the lone pair electrons of the N atom [17, 18]. Compared to TPA, *m*-MTDATA is a better  
44 electron donor and has higher thermal stability. The molecular plane of *m*-MTDATA can be defined by the four N atoms, i.e.  
45 (N)<sub>4</sub>-plane [17]. PPT (2,8-bis-(diphenyl-phosphoryl)-dibenzo[b,d]thiophene, C<sub>36</sub>H<sub>26</sub>O<sub>2</sub>P<sub>2</sub>S, shown in figure 1(b)) is an ambipolar  
46 acceptor material, used in combination with electron-donating materials to enhance the electroluminescence efficiency [19, 20].  
47 In this study, using Au(111) as substrate, we deposited *m*-MTDATA (donor) on top of a thick film (approx. four layers) of PPT  
48 (acceptor) and constructed a donor–acceptor molecular vertical heterostructure, used to shed light on the interfacial electronic  
49 structure modifications of *m*-MTDATA. An illustration of how this interface might look like is provided in figure 1(c). The  
50 comparison between different *m*-MTDATA depositions (i.e., monolayer-ML and submonolayer-subML) on PPT reveals, at  
51 subML coverage, a strong modification of the *m*-MTDATA molecular electronic structure, ascribed to a donor–acceptor  
52 hybridization due to the interaction within the resulting *m*-MTDATA/PPT heterostructure.

## 53 2. Methods

54 The synchrotron radiation-based photoelectron spectroscopy (PES) and near-edge x-ray absorption fine structure (NEXAFS)  
55 measurements were carried out at the materials science beamline of the Elettra synchrotron [21]. The PE spectra were recorded  
56 by the Specs Phoibos 150 hemispherical electron analyzer mounted at the end station. During the measurements, the base  
57 pressure of the analysis chamber was in the 10<sup>-10</sup> mbar range. All the samples were prepared with a base pressure of a high  
58 10<sup>-10</sup> mbar range. The Au(111) substrate was cleaned by repeated Ar<sup>+</sup> sputtering and annealing cycles until no contaminants were  
59 observed by the PE measurements.

60 The PPT/Au(111) heterostructure was prepared by thermal evaporation of PPT (Lumtec, purity > 99%) at 205 °C from a quartz  
61 crucible, heated by a tantalum wire, onto the clean Au(111). The thickness of the PPT thick film was controlled by the  
62 evaporation time and was estimated at about 11.3 Å (i.e., approximately 4 ML) by the attenuation of the PES Au 4f lines [22].  
63 Then the *m*-MTDATA/PPT/Au(111) heterostructure was prepared by depositing *m*-MTDATA (Sigma Aldrich, purity 98%) onto  
64 the PPT film via thermal evaporation at 190 °C from a similar Knudsen type evaporator as used for the PPT evaporation. Two  
65 thicknesses of *m*-MTDATA were prepared, corresponding to subML (approx. 0.5 ML) and 1 ML, respectively.  
66 The C 1s and N 1s core level PE spectra were measured at normal emission (NE) to the electron analyzer using photon energies  
67 of 392 and 495 eV, respectively. The resolutions were about 330, 430, and 150 meV for C 1s, N 1s and VB measurements,  
68 respectively. The NEXAFS spectra at the C and N K-edges of the deposited molecules were recorded using partial Auger yield.  
69 The measurements were performed at different scattering geometries: normal incidence (NI, 90° between the incident light and  
70 the surface plane), normal emission (NE, 90° between the analyzer and the surface plane, or 60° between the incident light and

71 the surface plane) and grazing incidence (GI,  $10^\circ$ , between the incident light and the surface plane). The photon energy scales of  
72 the NEXAFS were calibrated measuring the Au 4f PES lines by the 1st and 2nd order light. The energy resolution for the C and  
73 N K-edge NEXAFS spectra was estimated to be about 250 and 400 meV, respectively. Other experiment details can be found in  
74 reference [23].

### 75 3. Results and discussions

76 The C 1s PES results of *m*-MTDATA/PPT/Au(111) are shown in figure 2(a). The PPT/Au(111) spectrum shows a symmetric  
77 peak centered at 285.15 eV binding energy (BE) with FWHM about 0.68 eV. The C 1s peak becomes slightly asymmetric and  
78 shifted toward higher BE with subML *m*-MTDATA coverage (285.30 eV, FWHM = 0.75 eV). The C1s peak shifts further at 1  
79 ML *m*-MTDATA coverage (main peak at about 285.40 eV), and a shoulder appears at the higher BE side (286.40 eV, indicated  
80 by the blue arrow in figure 1(a)). Comparing to the gas phase *m*-MTDATA results [17], the shoulder feature at 1 ML *m*-  
81 MTDATA coverage can be attributed to the contribution from *ipso* ( $-\text{C}-\text{N}-$ ) and methyl ( $-\text{CH}_3$ ) type carbon of *m*-MTDATA.  
82 Since nitrogen is only present in *m*-MTDATA, we can visualize and confirm the *m*-MTDATA growth process by the N 1s PES  
83 measurements, shown in figure 2(b). The PPT/Au(111) substrate shows no N contribution and we find a broad N 1s peak  
84 centered at about 400.20 eV with FWHM = 1.20 eV of subML *m*-MTDATA/PPT. When the thickness of *m*-MTDATA reaches 1  
85 ML the N 1s peak also shifts to higher BE (at 400.40 eV) with a FWHM of 1.20 eV. A similar shift to higher BE was also  
86 observed for *m*-MTDATA on Au(111), without PPT [23]. We note that similar shifts (for example C 1s and N 1s) toward higher  
87 BE with increasing thickness are quite common in organic films [24]. This kind of shift is usually ascribed to the decreased  
88 surface screening of the core hole in PES. The same trend of the shift toward higher BE can still be observed in very thick films  
89 (up to 100 Å) [25].

90 The valence band (VB) PES results of *m*-MTDATA/PPT are shown in figure 2(c), measured with 100 eV photon energy. At  
91 subML *m*-MTDATA coverage on PPT, only little changes can be observed, whereas at 1 ML *m*-MTDATA coverage, although  
92 the VB PES is still dominated by the PPT electronic states, we observe the appearance of the HOMO features and of another  
93 small feature (at 12.00 eV BE), indicated by the blue arrows in the figure.

94 For increasing the surface sensitivity of the valence measurements and then better resolve the *m*-MTDATA spectroscopic  
95 features, we used a photon energy of 40 eV (figure 1(d)). To easily locate the *m*-MTDATA electronic states, we also show the  
96 gas phase *m*-MTDATA valence PES measured at the same photon energy (green markers, shifted  $-4.6$  eV) [17]. From this  
97 comparison, we clearly see the HOMO contribution from the *m*-MTDATA in the *m*-MTDATA/PPT/Au(111) structure,  
98 reasonable since *m*-MTDATA is a donor molecule. Although the characteristic three-peak outermost valence feature of *m*-  
99 MTDATA is not resolved due to the solid-state effect [23, 26], with the help of the gas phase result we can still identify the  
100 HOMO at about 1.55 eV. Moreover, the small feature at 11.90 eV is also a contribution by the *m*-MTDATA.

101 To understand the molecular arrangement of *m*-MTDATA when adsorbed onto PPT, we carried out polarization-dependent  
102 NEXAFS measurements for each *m*-MTDATA coverage (subML and 1 ML, respectively). This method consists of making  
103 NEXAFS measurements at different orientations of the sample with respect to the incident light. The molecular orientation can  
104 be extracted from the absorption spectra as a function of the angle  $\theta$  formed by the surface plane with respect to the linearly  
105 polarized electric field of the photon beam [25]. Therefore, in general, the resonances are expected to be enhanced when the light  
106 polarization vector ( $E$  vector) is aligned along the direction of maximum amplitude of the final state orbital. Considering the N  
107 K-edge of *m*-MTDATA, the  $\pi^*$  resonance intensity is expected to be most intensive when the  $E$  vector is perpendicular to the  
108 molecular plane, i.e.  $(\text{N})_s$ -plane, and to vanish when the polarization is parallel to the molecular plane [24]. Details of the  
109 discussions and illustrations of the deposited *m*-MTDATA molecular plane can be found in our recent *m*-MTDATA/Au(111)  
110 study [23].

111 The polarization-dependent C K-edge NEXAFS results are shown in figure 3, measured at GI and NI angles. It is no surprise to  
112 see that there is no evident polarization dependency in *m*-MTDATA/PPT/Au(111). With increasing *m*-MTDATA thickness, the  
113 C K-edge NEXAFS results still show no polarization dependency. In fact, all of the carbon atoms (in total 93 C atoms) from PPT  
114 and *m*-MTDATA (both of quite complex molecular structure), contribute to the C K-edge signal. We, therefore, cannot draw any  
115 conclusion about the molecular orientation and we just suggest that the molecules can have a quite complex/disordered  
116 arrangement.

117 To look closer at the modifications of the absorption spectra for increasing *m*-MTDATA coverage onto PPT, we zoom into the  
118 photon energy region of the main absorption resonance of the C K-edge NEXAFS (figure 3(b)). The main absorption peak of the  
119 C K-edge NEXAFS is found at about 285.00 eV for both subML *m*-MTDATA and 1 ML *m*-MTDATA coverage and also for  
120 PPT/Au(111). For increasing *m*-MTDATA coverage, the intensity of the peak at about 286.20 eV (i.e., about 1 eV from the main  
121 resonance) is enhanced. This peak is absent in C K-edge results of PPT in gas phase [19] and of the PPT thick film. By  
122 comparing to the gas phase and calculated *m*-MTDATA C K-edge NEXAFS results [17], the peak at about 286.20 eV is ascribed  
123 to the *ipso*-kind C atoms of the *m*-MTDATA molecule.

124 The N K-edge NEXAFS results of *m*-MTDATA/PPT are shown in figure 4. Unlike the C K-edge NEXAFS spectra that are the  
125 result from all C atoms from both *m*-MTDATA and PPT, only the four N atoms of the *m*-MTDATA molecule contribute to the N  
126 K-edge NEXAFS. Considering the molecular structure with the planes defined by the N atoms and the *ipso* carbons bonded to the  
127 nitrogens, we could be able to determine the arrangement of *m*-MTDATA from the N K-edge NEXAFS results. The analysis was  
128 focused on the prominent  $\pi^*$  structure, which corresponds to a transition into an empty N state oriented out of the molecular plane  
129 at 402.45 eV photon energy for the subML and 402.50 eV for the 1 ML *m*-MTDATA/PPT, respectively. From figure 4 we can  
130 find that, at the subML *m*-MTDATA/PPT coverage, the  $\pi^*$  resonance at 402.45 eV is enhanced at GI angle. Its intensity becomes  
131 much less sensitive to the polarization for increased molecular coverage (figure 4 upper panel). The results suggest that, at  
132 subML *m*-MTDATA/PPT, the N planes (formed by the four nitrogen atoms) of the *m*-MTDATA molecule would prefer to stay  
133 quite parallel to the substrate. However, it is important to consider the results as only indicating a trend, because the molecules  
134 are adsorbed on a PPT film and not on a flat substrate which can of course imply quite complex and diverse molecular  
135 arrangements. At 1 ML *m*-MTDATA/PPT, there is no polarization variation of the  $\pi^*$  resonance intensity for the different  
136 experimental set-ups, indicating that the arrangement of *m*-MTDATA molecules becomes more disordered.

137 Another important finding is that at subML *m*-MTDATA/PPT, there is a new pre-edge feature starting at 399 eV photon energy,  
138 quite similar to the pre-edge at the interface of *m*-MTDATA/Au(111) attributed to the *m*-MTDATA-Au hybridization state [23].  
139 However, in our case, the *m*-MTDATA molecules are adsorbed on a thick PPT film that breaks the interaction between *m*-  
140 MTDATA and Au(111). This is confirmed by figures 2(c) and (d) where the Au substrate photoemission lines are not visible in  
141 the PPT film spectra, indicating that the PPT thickness is larger than the escape depth of the Au photoelectron. Then we can  
142 regard these new states as formed by the interaction at the interface between the organic donor *m*-MTDATA and the organic  
143 acceptor PPT. On the other hand, there is no pre-edge feature at the 1 ML *m*-MTDATA/PPT/Au(111) supporting that these states  
144 are the results of the interaction at the organic donor-acceptor interface. In view of the molecular arrangement, changing from a  
145 quite defined orientation trend to a more disordered adsorption from subML to 1 ML *m*-MTDATA/PPT/Au(111), we can  
146 speculate that this pre-edge feature (and then the interface interaction) could be related to the molecular arrangement between *m*-  
147 MTDATA and PPT, i.e. the interaction could promote the adsorbate arrangement, and/or vice versa.

148 The energy position of the pre-edge feature, indicates, as already investigated for *m*-MTDATA/Au(111) that new hybrid states  
149 are available in the original molecular gap [23]. This is a crucial modification of the electronic structure at such an interface,  
150 because it can represent a new channel for delocalization of the excited electrons from the donor to the acceptor molecule. This  
151 new hybrid state provides an important insight to the D-A charge-transfer dynamics. Further ongoing investigations by means of  
152 resonance photoelectron spectroscopy and core-hole clock method will complete our spectroscopic results.

## 153 4. Conclusion

154 We successfully prepared *m*-MTDATA/PPT/Au(111) donor–acceptor vertical heterostructures. N K-edge NEXAFS shows that,  
155 at subML *m*-MTDATA/PPT/Au(111), the N-planes of the *m*-MTDATA molecules seem to prefer to arrange quite parallel to the  
156 surface. The molecular adsorbate becomes more disordered at 1 ML *m*-MTDATA/PPT/Au(111). The electronic structure of *m*-  
157 MTDATA in the subML *m*-MTDATA/PPT/Au sample undergoes important modifications as evidenced by the appearance of a  
158 pre-edge feature in the N K-edge spectrum. This pre-edge feature is ascribed to new hybrid states formed at the donor–acceptor  
159 interface, i.e. between *m*-MTDATA and PPT film. These findings and our previous study of *m*-MTDATA/Au(111) prove that *m*-  
160 MTDATA can form hybridization states between both organic–metal and organic–organic interfaces, with a consequent impact in  
161 donor–acceptor electronic devices. We believe that the new hybridized states at the organic–organic interface could  
162 promote/facilitate the charge transfer process and further electron dynamics studies are planned to fully elucidate this question.

## 163 Acknowledgments

164 TZ thanks the financial support from the National Natural Science Foundation of China (Nos. 61901038, 61971035, 61725107,  
165 92163206), Beijing Natural Science Foundation (Nos. Z190006, 4192054), National Key Research and Development Program of  
166 China (2020YFA0308800, 2019YFA0308000), the support from the Beijing Institute of Technology Research Fund Program for  
167 Young Scholars and the Vice-Chancellor of Uppsala University for financial support through the U4 collaboration. BB  
168 acknowledges the Swedish Research Council for research Grant (VR 2014-3776). FOLJ acknowledges support from the Swedish  
169 Research Council (Grants VR 2014-6463 and 2020-06409). The authors acknowledge the EU CERIC-ERIC Consortium for the  
170 access to experimental facilities and financial support. We thank the staffs at Materials Science beam line, at Elettra, for all the  
171 help provided during the beamtimes. We thank G Bortoletto and C Pedersini of the User Support Lab at Elettra.

## 172 References

- 173 [1]Deotare P B et al. 2015 Nanoscale transport of charge-transfer states in organic donor–acceptor blends Nat.  
174 Mater. 14 1130–4
- 175 [2]Goushi K and Adachi C 2012 Efficient organic light-emitting diodes through up-conversion from triplet to singlet  
176 excited states of exciplexes Appl. Phys. Lett. 101 023306
- 177 [3]Wang S, Wang X, Yao B, Zhang B, Ding J, Xie Z and Wang L 2015 Solution-processed phosphorescent organic  
178 light-emitting diodes with ultralow driving voltage and very high power efficiency Sci. Rep. 5 12487
- 179 [4]Johansson E M J, Odelius M, Karlsson P G, Siegbahn H, Sandell A and Rensmo H 2008 Interface electronic  
180 states and molecular structure of a triarylamine based hole conductor on rutile TiO<sub>2</sub>(110) J. Chem. Phys. 128 184709
- 181 [5]Johansson E M J, Karlsson P G, Hedlund M, Ryan D, Siegbahn H and Rensmo H 2007 Photovoltaic and  
182 interfacial properties of heterojunctions containing dye-sensitized dense TiO<sub>2</sub> and tri-arylamine derivatives Chem.  
183 Mater. 19 2071–8
- 184 [6]Kabe R and Adachi C 2017 Organic long persistent luminescence Nature 550 384–7

185 [7]Wang J, Liu K, Ma L and Zhan X 2016 Triarylamine: versatile platform for organic, dye-sensitized, and  
186 perovskite solar cells *Chem. Rev.* 116 14675–725

187 [8]Jailaubekov A E et al. 2013 Hot charge-transfer excitons set the time limit for charge separation at donor/acceptor  
188 interfaces in organic photovoltaics *Nat. Mater.* 12 66–73

189 [9]Vandewal K et al. 2014 Efficient charge generation by relaxed charge-transfer states at organic interfaces *Nat.*  
190 *Mater.* 13 63–8

191 [10]Gélinas S, Rao A, Kumar A, Smith S L, Chin A W, Clark J, van der Poll T S, Bazan G C and Friend R H 2014  
192 Ultrafast long-range charge separation in organic semiconductor photovoltaic diodes *Science* 343 512–6

193 [11]Johansson F O L, Ivanović M, Svanström S, Cappel U B, Peisert H, Chassé T and Lindblad A 2018  
194 Femtosecond and attosecond electron-transfer dynamics in PCPDTBT:PCBM bulk heterojunctions *J. Phys. Chem C*  
195 122 12605–14

196 [12]Saadon A K and Al-agealy H J M 2020 Study of photoemission and electronic properties of dye-sensitized solar  
197 cells *Energy Rep.* 6 28–35

198 [13]Wu J-H, Chen W-C and Liou G-S 2016 Triphenylamine-based luminogens and fluorescent polyimides: effects  
199 of functional groups and substituents on photophysical behaviors *Polym. Chem.* 7 1569–76

200 [14]Chiba T, Pu Y-J, Kido J, Watanabe Y and Kido J 2018 White OLED (WOLED) and charge generation layer  
201 (CGL) *Sci. Rep.* 8 1–22

202 [15]Agarwala P and Kabra D 2017 A review on triphenylamine (TPA) based organic hole transport materials  
203 (HTMS) for dye sensitized solar cells (DSSCS) and perovskite solar cells (PSCS): evolution and molecular  
204 engineering *J. Mater. Chem. A* 5 1348–73

205 [16]Zhang T et al. 2017 Conclusively addressing the COPC electronic structure: a joint gas-phase and solid-state  
206 photoemission and absorption spectroscopy study *J. Phys. Chem C* 121 26372–8

207 [17]Zhang T et al. 2019 Electronic structure modifications induced by increased molecular complexity: from  
208 triphenylamine to m-MTDATA *Phys. Chem. Chem. Phys.* 21 17959–70

209 [18]Zhang T et al. 2018 Lone-pair delocalization effects within electron donor molecules: the case of triphenylamine  
210 and its thiophene-analog *J. Phys. Chem C* 122 17706–17

211 [19]Guarnaccio A et al. 2020 PPT isolated molecule and its building block moieties studied by C 1s and O 1s gas  
212 phase x-ray photoelectron and photoabsorption spectroscopies *J. Phys. Chem C* 124 9774–86

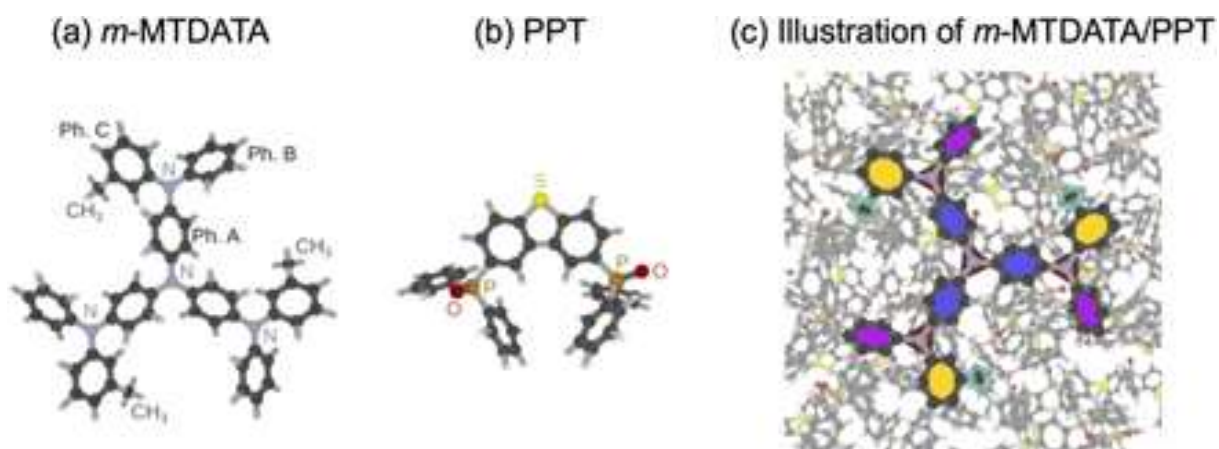
213 [20]Bernes E et al. 2020 S 2p and P 2p core level spectroscopy of PPT ambipolar material and its building block  
214 moieties *J. Phys. Chem C* 124 14510–20

215 [21]Zhang T et al. 2022 Clarifying the adsorption of triphenylamine on Au(111): filling the HOMO–LUMO gap *J.*  
216 *Phys. Chem C* 126 1635–43

217 [22]Graber T, Forster F, Schöll A and Reinert F 2011 Experimental determination of the attenuation length of  
218 electrons in organic molecular solids: the example of PTCDA *Surf. Sci.* 605 878–82

219 [23]Zhang T et al. 2022 m-MTDATA on Au(111): spectroscopic evidence of molecule-substrate interactions *J.*  
220 *Phys. Chem C* 126 3202

- 221 [24]Zhang T et al. 2021 Spectroscopic evidence of new low-dimensional planar carbon allotropes based on  
222 biphenylene via on-surface Ullmann coupling *Chemistry* 3 1057–62
- 223 [25]Totani R et al. 2017 Electronic structure investigation of biphenylene films *J. Chem. Phys.* 146 054705
- 224 [26]Tillborg H, Nilsson A and Mårtensson N 1993 Shake-up and shake-off structures in core level photoemission  
225 spectra from adsorbates *J. Electron Spectrosc. Relat. Phenom.* 62 73–93

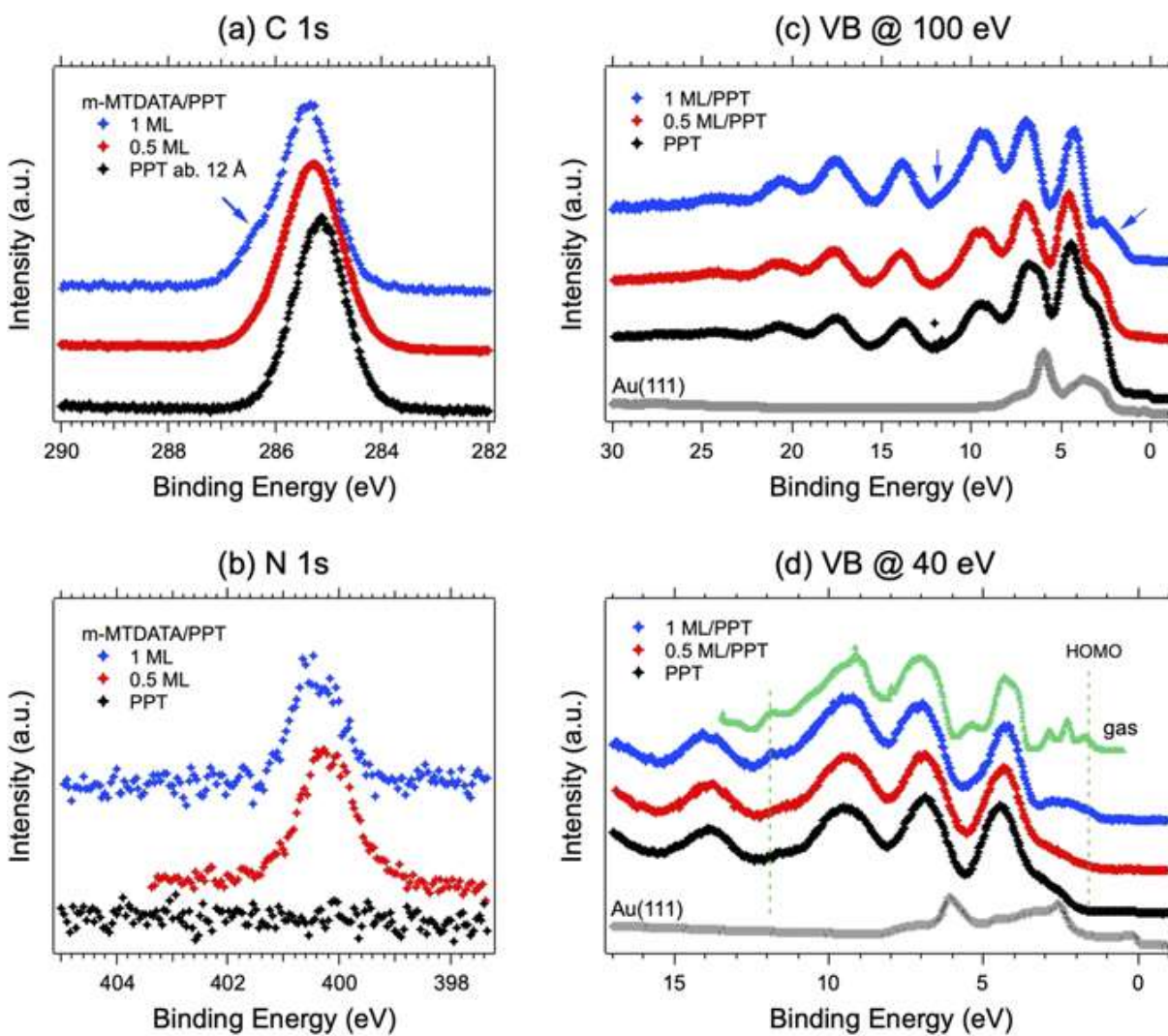


227

228

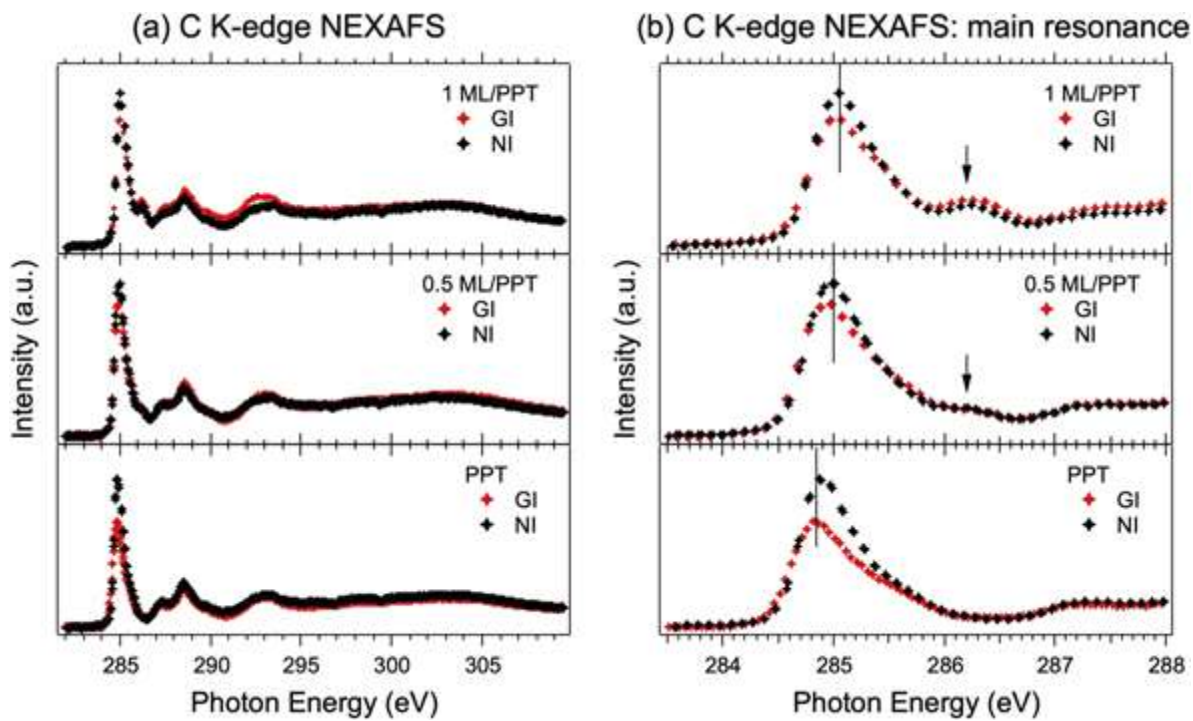
Figure 1. Structure of (a) *m*-MTDATA and (b) PPT. An illustration of a possible *m*-MTDATA/PPT interface is shown in (c).





230

231 **Figure 2.** PES results of (a) C 1s core level, (b) N 1s core level, (c) VB measured at 100 eV photon energy and (d) VB measured232 at 40 eV, comparing different thicknesses of *m*-MTDATA on PPT/Au(111).



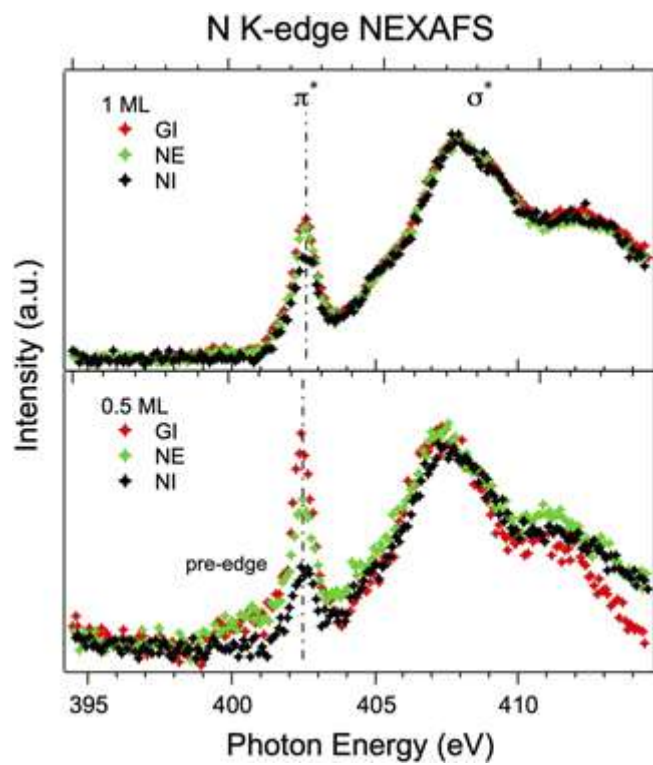
233

234

235

236

Figure 3. (a) Polarization dependent C K-edge NEXAFS results of *m*-MTDATA/PPT/Au(111) for different coverage from PPT thick film, subML to 1 ML. (b) Zoom-in of (a) to enlarge the main resonance energy region. The black bars indicate the position of the main resonance. The arrows point to the contribution from *ipso*-kind C atoms from *m*-MTDATA molecule.



237

238

239

**Figure 4.** Polarization dependent N K-edge NEXAFS results of *m*-MTDATA/PPT with different coverages. The intensities are normalized to the  $\sigma^*$  to enhance the  $\pi^*$  polarization dependence.